Food Chemistry: X 24 (2024) 101996

Contents lists available at ScienceDirect

Food Chemistry: X

journal homepage: www.sciencedirect.com/journal/food-chemistry-x

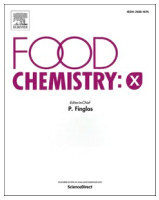

Soluble and insoluble dietary fiber at different ratios: Hydration characteristics, rheological properties, and ameliorative effects on constipation

Lijuan Wang [a,c], Jiaxin Wang [a], Jialin Wang [a,d], Zicong Guo [a], Zaigui Li [a], Ju Qiu [a,*], Lili Wang [b,*]

[a] Department of Nutrition and Health, China Agricultural University, No.17 Tsinghua East Road, Haidian District, Beijing 100083, PR China
[b] Institute of Food Science and Technology, Chinese Academy of Agricultural Sciences, Ministry of Agriculture, No. 2, Yuan Ming Yuan West Road, Haidian District, Beijing 100193, PR China
[c] Food Laboratory of Zhongyuan, Intersection of Wenming Road and 107 National Road, Yancheng District, Luohe City, Henan Province 462044, PR China
[d] State Key Laboratory of Food Nutrition and Safety, College of Food Science and Engineering, Tianjin University of Science and Technology, Tianjin 300457, PR China

ARTICLE INFO

Keywords:
Soluble dietary fiber
Insoluble dietary fiber
Proportions
Hydration characteristic
Constipation

ABSTRACT

The proportion of soluble components in dietary fiber is an important factor affecting its physicochemical properties and physiological functions. The influence mechanisms of insoluble (IDF) and soluble dietary fiber (SDF) at different ratios on constipation were investigated. Results showed that SDF had higher active groups and water swelling capacity than IDF. The viscosity of chyme with SDF alone was the highest in oral and gastric phases. The gastric emptying rate and small intestine propulsion capacity increased significantly, especially when IDF/SDF was 1:1. IDF and a lower proportion of SDF (< 50 %) promoted gut microbiota diversity and short-chain fatty acids production. The contents of 5-hydroxytryptamine, acetylcholinesterase and gastrin reached the maximum value when the IDF ratio was 50 %. In conclusion, IDF could act synergistically with SDF to promote defecation and relieve constipation, and the effect was the best when the ratio of IDF to SDF was 1:1.

1. Introduction

Constipation is one of the most common gastrointestinal disorders, with a global prevalence of about 15 % (Bharucha & Lacy, 2020). Chronic constipation is of great harm, and may induce toxemia, neurological disorders, metabolic disorders, colon cancer and other diseases (Sumida et al., 2019). Lubricants (opiates), stimulants (lubiprostone, linaclotide), and osmotic and stimulant laxatives (bisacodyl, polyethylene glycol 4000 dispersion) are commonly used in the treatment of constipation (Sharma & Rao, 2017). However, these drugs not only have poor efficacy and strong drug dependence (Novick et al., 2002), but also have more adverse effects, such as diarrhea, abdominal pain, flatulence, nausea, and headache. Moreover, some drugs may also increase the risk of coronary heart disease and ischemic stroke (Sharma & Rao, 2017). Therefore, dietary therapy is becoming more and more popular for the treatment of constipation because of its safety. Many studies have shown that foods rich in dietary fiber (DF), such as whole grain, fruits and vegetables, can relieve constipation to varying degrees (Bae, 2014).

DF is the remnants of the edible part of plants and analogous carbohydrates that are resistant to digestion and absorption in the human small intestine, but can be fully or partially fermented in the large intestine. According to the solubility in water, DF can be divided into two categories: soluble DF (SDF) and insoluble DF (IDF). The proportion of soluble components in dietary fiber is an important factor affecting its physicochemical properties and physiological functions. Due to its relatively orderly structure arrangement, IDF has poor solubility, low viscosity, and poor adsorption capacity for substances such as glucose, harmful ions and nitrite. Compared with IDF, SDF has better hydration properties, oil adsorption capacity, ion exchange capacity and

Abbreviation: IDF, insoluble dietary fiber; SDF, soluble dietary fiber; DF, dietary fiber; WRC, water retention capacity; WSI, water solubility index; WSC, water swelling capacity; SSF, Simulated Salivary Fluid; SGF, Simulated Gastric Fluid; SIF, Simulated Intestinal Fluid; SEM, Scanning electron microscope; FTIR, Fourier transformed infrared spectroscopy; CT, Control team group; MC, Model control group; PEG, Positive control group (polyethylene glycol 4000 powder); 4I-1S, IDF: SDF = 4: 1; 2I-1S, IDF: SDF = 2: 1; 1I-1S, IDF: SDF = 1: 1; SCFAs, short-chain fatty acids; 5-HT, 5-hydroxytryptamine; AchE, acetylcholinesterase; MTL, gastrin; NO, nitric oxide.

* Corresponding authors.
E-mail addresses: wanglijuan2023@cau.edu.cn (L. Wang), qiuju@cau.edu.cn (J. Qiu), wlland2013@163.com (L. Wang).

https://doi.org/10.1016/j.fochx.2024.101996
Received 31 July 2024; Received in revised form 4 November 2024; Accepted 11 November 2024
Available online 13 November 2024

antioxidant ability, because SDF contains irregular main and side chain structure. SDF and IDF have some either similar or different physiological functions (Jiménez-Escrig & Sánchez-Muniz, 2000). Both IDF and SDF have a positive effect in relieving constipation and maintaining intestinal health through volume expansion, fermentation and metabolism regulation (Sharma & Rao, 2017; Slavin, 2013). However, the low content of SDF in natural DF limits its physiological activity and affects its application in food. At present, the effect of increasing the proportion of SDF in DF on the physicochemical properties and physiological functions of DF is still lacking.

Cereals (*e.g.* wheat, oats, and black barley) are rich in both IDF and SDF, and are usually consumed as staple foods in most countries, which typically contribute about the main source DF intake. The DF in cereals is mainly IDF, accounts for more than 50–80 % in most cases. Wheat bran is a concentrated source of IDF and mainly consists of cellulose, lignin, and arabinoxylan (Rosa-Sibakov et al., 2015). IDF made from wheat bran has an effect on gastrointestinal function. The wheat bran can increase fecal bulk through their ability to bind water in a network of fibers and thus modulate the intestinal transit time (Saini et al., 2023). In human experiments, the intake of wheat bran extract increased fecal *Bifidobacterium*, decreased microbial diversity and softened stool consistency (Müller, Hermes, Emanuel E, Holst, Zoetendal, Smidt, et al., 2020). β-glucan is a representative SDF, which is mainly derived from oats or barley in cereals. β-glucan has good water absorption, swelling and water retention capacity, which can increase feces weight and delay gastric emptying (Mälkki & Virtanen, 2001). Meanwhile, β-glucan can be fermented by colonic microorganisms to produce a higher proportion of short-chain fatty acids (SCFAs), which lowers intestinal pH, promotes intestinal peristalsis, and thus improves intestinal health (Yang et al., 2013). The intake of foods with high content of both SDF and IDF is more beneficial than DF supplied alone in relieving symptoms in patients with constipation (Chan et al., 2007; Jung et al., 2020). However, the effect of IDF and SDF at different ratios on constipation is still lack of research.

It was hypothesized that DF of a certain proportion of SDF and IDF had better physicochemical and physiological properties than SDF or IDF alone. In this study, IDF prepared from wheat bran was mixed with SDF of β-glucan from oat at different ratios. The effects of different ratios of IDF and SDF on constipation in mice were investigated through hydration properties, chyme rheological properties, gastrointestinal motility, intestinal flora, short chain fatty acid, and gastrointestinal hormone. The purpose of the study is to provide scientific guidance for the DF dietary therapy of constipation.

2. Materials and methods

2.1. Materials and reagents

Wheat bran, China-Italian Agricultural Development Ltd. (Shanxi, China). β-glucan, Wongyuan Guangye Qingyi Food Technology Ltd. (SDF content 77.70 %) (Guangdong, China). Total DF assay kit, total starch assay kit and β-glucan assay kit were purchased from Megazyme (Megazyme International Ireland Ltd., Bray, Ireland). Amylase (≥5 u/mg), trypsin (≥2500 u/mg), and glucosidase (≥700 u/μL) were purchased from Shanghai Yuanye Biotechnology Ltd. (Shanghai, China). Loperamide hydrochloride and polyethylene glycol 4000 dispersion was purchased from Xi'an Janssen Pharmaceutical Ltd. (Shanxi, China). Elisa kits of gastric actin (MTL), 5-Hydroxytryptamine (5-HT), and acetylcholinesterase (AChE) were purchased from Jiangsu Jingmei Biotechnology Ltd. (Jiangsu, China). Other reagents were analytical grade and purchased from Sinopharm Group Chemical Reagent Ltd. (Shanghai, China).

2.2. Preparation of IDF

The IDF was prepared according to the following method: Wheat bran (80 g) and hexane (200 mL) was mixed and stirred every 15 min to soak. After soaked for 2 h, the mixture was centrifuged at 1000 ×*g* for 10 min (25 °C) to remove the hexane. The precipitate was dispersed in 800 mL of deionized water and added with 1 g of amylase. The suspension was stirred at 65 °C for 2.5 h. Then it was cooled to 40 °C, adjusted the pH at 4, and incubated with glucosidase (0.035 mL) for 2.5 h. Thereafter, the pH was adjusted to 8, protease (0.35 g) was added and incubated at 55 °C for 2.5 h to remove starch and protein. The suspension was centrifugated at 1000 ×g for 10 min and the obtained residue was washed 3–5 times and freeze dried. The washing procedure was as follows: Residue was dispersed in 500 mL of deionized water, and the suspension was stirred for 5 min. Then, the suspension was centrifugated at 1000 ×g for 10 min to obtain the washed IDF residue. The whole washing procedure was repeated for 3–5 times.

The nutritional compositions of the prepared IDF and the purchased SDF were determined as follows: The total dietary fiber (TDF) and β-glucan content of samples were determined using a total dietary fiber assay kit and a Beta-Glucan test kit (KTDFR; Megazyme International Ireland Ltd., Bray, Ireland), respectively. Total starch (method 76–12), protein (method 46–10), crude fat (method 30–25), ash (method 08–01), and moisture (method 44–15) contents were measured according to AACC Approved Methods (American Association of Cereal Chemists (AACC), 2010). The results are shown in Table S1. The purity of IDF and SDF was about 88.04 % and 77.7 %, respectively. The total content of starch, protein and fat, were less than 5 %. The IDF and SDF were mixed at the ratio of 1:0, 4:1, 2:1, 1:1 and 0:1 based on the IDF and SDF content, respectively, to produce DF with different ratios for experiments.

2.3. Structural characteristic of DF

2.3.1. Scanning electron microscope (SEM)

The microstructure of IDF and SDF was observed by a scanning electron microscope (SEM, SU8020, Hitachi Ltd., Tokyo, Japan). Samples were mounted on a metal stub using double-sided adhesive tape and covered with 20 nm gold. Observations were conducted at an accelerating voltage of 5 kV, and photographed at magnifications of 500 × and 2000 × .

2.3.2. Fourier transformed infrared spectroscopy (FTIR) analysis

FTIR analysis of the IDF and SDF samples were performed using an FTIR spectrometer (Spectrum 100, PerkinElmer Co., USA) according to a prior method with minor modifications (Wang et al., 2021). DF samples and KBr powders were dried at 50 °C for 6 h. The samples were ground evenly with KBr at a ratio of 1: 100 (w: w). Then the mixture was pressed into transparent flakes, which were scanned in a wavenumber range of 400–4000 cm^{-1} with 4 cm^{-1} resolution and 32 times of scan.

2.4. Physicochemical properties of IDF and SDF at different ratios

2.4.1. Water retention capacity and water solubility index

The water retention capacity (WRC) and water solubility index (WSI) of DF with different ratios were determined by the method of Kurek et al. (2018) with some modifications. DF 500 mg (M) was hydrated in 20 mL of deionized water for 24 h at room temperature, and centrifuged at 4000 ×*g* for 10 min. The supernatant was collected and dried to constant weight (M_1). The residues were weighed and recorded as M_2. The WRC (g/g) and WSI (g/g) were calculated by the following formula:

$$\text{WRC (g/g)} = (M_2 - M)/M \quad (1)$$

$$\text{WSI (g/g)} = M_1/M \quad (2)$$

2.4.2. Water swelling capacity

The water swelling capacity (WSC) of DF with different ratios was determined according to the method of Sowbhagya et al. (2007). DF sample 500 mg (M) was loaded into a 15 mL centrifuge tube and its

volume was recorded as V_1. 10 mL of deionized water was mixed, and then left to stand at room temperature for 18 h. The volume of the solid fraction in the tube after standing was recorded as V_2 (the volume of non-supernatant liquid). The WSC (mL/g) was calculated according to the following formula:

$$\text{WSC (mL/g)} = (V_2 - V_1)/M \quad (3)$$

2.5. Effect of SDF and IDF at different ratios on rheological properties of chyme during in vitro digestion

The high DF animal feed was prepared by adding the mixture of IDF and SDF to the fiber free animal feed at a ratio of 10 %. The fiber free animal feed was prepared by removing DF from the standard animal feed. For preparation of oral, gastric and intestinal chyme, the *in vitro* method models upper GI tract digestion, including the oral phase, gastric phase and small intestine phase were carried out according to the method of Mäkelä et al. (2020) with slight modification. The Simulated Salivary Fluid (SSF), Simulated Gastric Fluid (SGF) and Simulated Intestinal Fluid (SIF) were prepared according to Table S2.

Oral phase: 3 g high DF feed samples were mixed with 2.1 mL SSF, and 15 μL 0.3 mol·L^{-1} $CaCl_2$ and 585 μL deionized water were added successively to adjust pH = 7. After preheating the above mixture to 37 °C, 0.3 mL salivary α-amylase solution (1500 U· mL^{-1}) was added to the mixture. The samples were mixed thoroughly and incubated at 37 °C for 2 min using a shaking incubator (BSD250, Shanghai Boxun Medical Biological Instrument Co. Ltd., Shanghai, China).

Gastric phase: After the oral phase, 4.5 mL SGF was added to the mixture and the pH was adjusted to 3.0 with 3 μL 0.3 mol·L^{-1} $CaCl_2$, 0.12 mL 1 mol·L^{-1} HCl, and 417 μL deionized water. Then, 0.96 mL of pepsin (25,000 U·mL^{-1}) was added, and the samples were mixed thoroughly and incubated at 37 °C for 30 min using a shaking incubator.

Small intestine phase: After the gastric phase, the sample was mixed with 6.6 mL SIF. The pH of the mixtures was adjusted to 7.0 with 24 μL 0.3 mol·L-1 $CaCl_2$, 0.09 mL 1 mol·L^{-1} NaOH, 0.786 mL deionized water, and 1.5 mL 160 mmol·L^{-1} bile salts. The samples were thoroughly mixed and incubated at 37 °C for 90 min using a shaking incubator.

The rheological properties of chyme were performed by an AR 2000 Rheometer (TA Instruments, New Castle, DE, USA). 1 mL chyme sample was placed in the center of the rheological platform with a diameter of 40 mm. The gap was set 1500 μm, and the shear rate was 0.1–100 s^{-1}. The test temperature was set at 37 °C.

2.6. Constipation mouse model

2.6.1. Experimental animals

The use of animals and experimental methods were in compliance with the National Institutes of Health Guidelines for the Care and Use of Laboratory Animals, approved by Xiamen Medical College (Permission number: 20220728004).

Eighty six-week-old healthy SPF male Balb/c mice (Shanghai Slaughter Laboratory Animal Co. Ltd., license No. 20170005045865) were maintained under SPF conditions and acclimatized for 7 days before experiments. During the acclimatization period, all mice were fed standard mouse chow (Beijing Nokongyuan Biotechnology Ltd.). The relative humidity was controlled between 50 % and 70 %, the temperature was controlled between 22 °C and 26 °C, and the circadian rhythm was 12 h daytime and 12 h nighttime.

2.6.2. Grouping and drug administration

After adaptation, mice were randomly divided into 8 groups: (1) Control team group (CT); (2) Model control group (MC); (3) Positive control group (polyethylene glycol 4000 powder, PEG); (4) IDF: SDF =1: 0 (IDF); (5) IDF: SDF = 4: 1 (4I—1S); (6) IDF: SDF = 2: 1 (2I—1S); (7) IDF: SDF = 1: 1 (1I—1S); (8) IDF: SDF =0: 1 (SDF). During the intervention period, the CT, MC and PEG groups were fed standard mouse chow, while the remaining groups were fed a 10 % DF replacement diet. Mice in each group (except CT group) were intragastric infused with loperamide 10 mg/kg daily for 14 days to establish constipation model. CT group was intragastric infused with the same dose of saline, and PEG group was given 3 g/kg PEG daily.

2.7. Fecal pellet count and water content

On the last morning of the intervention period, feces were collected from all mice within 2 h. The number of fecal pellets and the weight of wet feces (M_1) were recorded immediately after collection. Fecal pellets were dried at 60 °C for 12 h and weighed (M_2). Fecal water content (%) was calculated according to eq. (4) (Zhang, Zhong, et al., 2021):

$$\text{Fecal water content (\%)} = (M_1 - M_2)/M_1 \times 100 \quad (4)$$

2.8. Gastric emptying rate and small intestine propulsive capacity

At the end of the intervention period, all mice were fasted for 12 h. Each mouse was gavaged with 0.2 mL carbon meal (10 % suspension of activated carbon in 0.5 % carboxymethylcellulose). After 20 min of intragastric administration, the mice were anesthetized using carbon dioxide in a gradual fill method according to the EU Directive 2010/63. The flow rate of carbon dioxide was controlled at 20 % chamber air displacement per minute. The blood was collected from the ophthalmic venous plexus, and then the mice were sacrificed by cervical dislocation. The stomach (cardia to pylorus) was quickly removed and weighed (M_1). Then the stomach contents were washed with phosphate buffer (pH = 7.4), and the net weight of the stomach was weighed (M_2). The gastric emptying rate (%) was calculated according to eq. (5) (Crowe & Kinsey, 2017). Meanwhile, the intestinal tube (small intestine) with the upper end from the pylorus and the lower end to the ileocecal region was cut and placed on a white background plate. The small intestine was gently pulled into a straight line and the length of the intestinal tube was measured as L_1. The distance from the pylorus to the front of the black semi-solid paste was measured and recorded as L_2. The small intestine propulsive capacity (%) was calculated according to eq. (6) (Wang et al., 2017).

$$\text{Gastric emptying rate (\%)} = [1 - (M_1 - M_2)/M_1] \times 100 \quad (5)$$

$$\text{Small intestine propulsion capacity (\%)} = (L_2/L_1) \times 100 \quad (6)$$

2.9. Intestinal flora analysis

Intestinal flora of the colon contents (stored at −80 °C under liquid nitrogen freezing) were analyzed by OE biotech Co., Ltd. (Shanghai, China). The genomic DNA of the samples was first extracted by DNA extraction kit, and the concentration of DNA was detected by agarose gel electrophoresis and NanoDrop2000. The genomic DNA was used as template for PCR using specific primers with barcode to identify the 16S rDNA V3-V4 region (primers 343F and 798R) according to the selection of sequencing region. The PCR products were then detected by electrophoresis and purified using magnetic beads, and the purified products were used as second-round PCR templates, which were also amplified and purified. After purification, the PCR products were quantified, mixed in equal amounts according to the PCR product concentrations, and sequenced on the machine. The raw data were processed and analyzed using several software such as Trimmomatic software, FLASH software, Vsearch software, and QIIME software.

2.10. Determination of short-chain fatty acids (SCFAs)

About 100 mg cecum contents and 250 μL of ultrapure water was mixed by vortex for 1 min. Then 50 μL of 25 % metaphosphoric acid was added, and the mixture was vortexed for 30 s. After standing at 4 °C for

30 min, the samples were centrifuged at 5000 ×*g* for 15 min. The supernatant was collected, filtered through a 0.22 μm aqueous membrane and transferred to a brown injection vial (the above steps were performed on ice), and the content of SCFAs was determined by external standard method of gas chromatography.

2.11. Determination of 5-HT, AchE, MTL and NO

The blood samples were collected and stood for one hour at room temperature. Then, the blood samples were centrifuged at 3000 ×*g* for 10 min to obtain the serum. The levels of 5-hydroxytryptamine (5-HT), acetylcholinesterase (AchE), gastrin (MTL) and nitric oxide (NO) were measured according to the instructions of the ELISA kit.

2.12. Data analysis

The experimental data were expressed as mean ± standard deviation. SPSS 25.0 statistical software was used for data analysis and processing. One-way analysis of variance ANOVA was used to test the data for significant differences ($P < 0.05$) by Duncan's multiple comparison method. Origin 2019b software was used for plotting.

3. Results and discussion

3.1. Microstructure characteristics of IDF and SDF samples

The micromorphology of IDF and SDF samples was observed by SEM under 500 × and 2000 × magnifications. As shown in Fig. 1A, the IDF sample had a uniform plate-like structure with a smooth surface and almost no wrinkles. It was found that there were some pores between the small layers of IDF at the magnification of 2000 × (Fig. 1B). The pores were consisted mainly of tissue-level and cellular-level pores as well as particle interstices (Li et al., 2022), which was closely related to the hydration characteristics of IDF. The SDF was loosely agglomerated due to its certain viscosity (Fig. 1C). The surface of SDF was irregular, and the pore structures were also found in SDF aggregates (Fig. 1D). Compared with IDF, the fibrous structure of SDF was looser and more porous, which might expose more polar groups.

3.2. Molecular structure of IDF and SDF samples

FTIR was able to identify the information of molecular bond vibrations and could be a tool for understanding changes in the molecular structure. The infrared spectra of IDF and SDF are shown in Fig. 1E. It was notable that the IDF and SDF samples both had broad bands around 3410 cm^{-1} and 1072 cm^{-1}, which were caused by O—H stretching

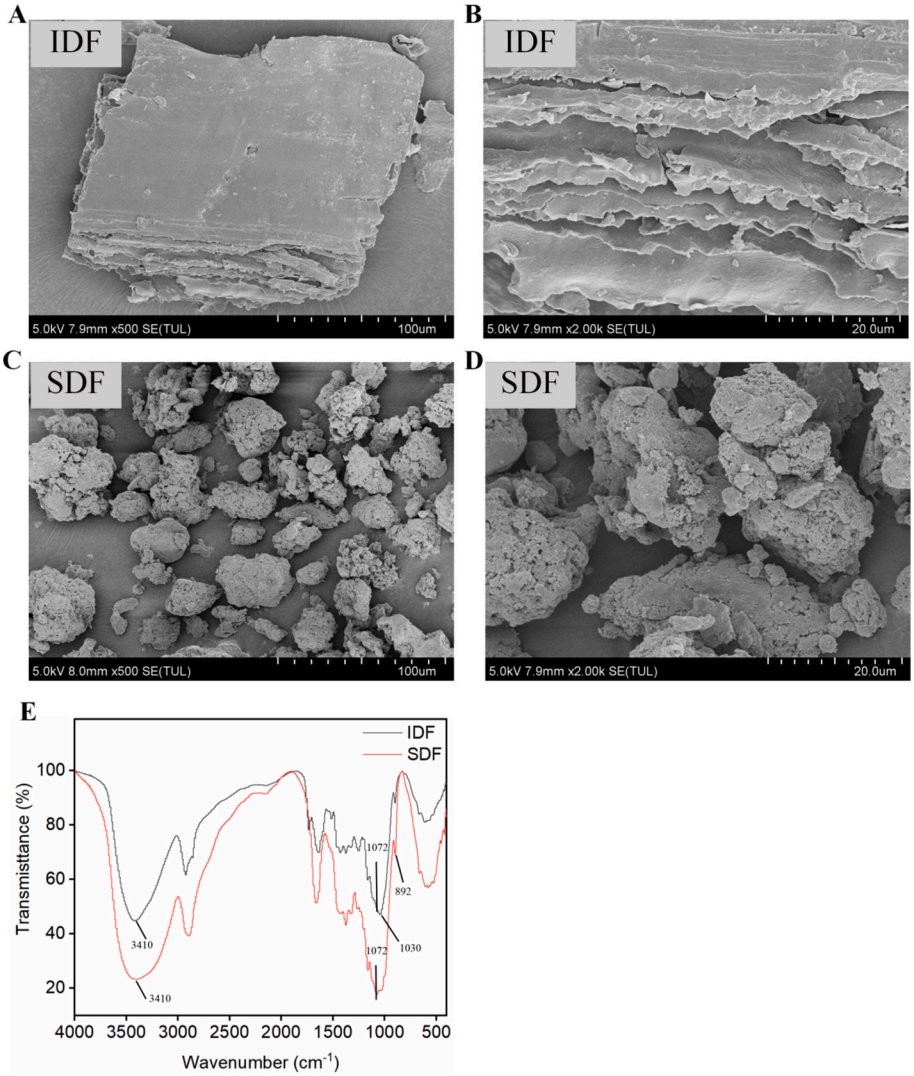

Fig. 1. Scanning electron microscopy images (A-D) and Fourier transformed infrared spectrum (E) of IDF and SDF.

(Rezvani & Goli, 2023). The peak near 1030 cm^{-1} of IDF could be presented as C—O stretching vibration of hemicellulose and lignin pyranose ring (Kanwar et al., 2023). The small peak around 892 cm^{-1} of SDF was related to the bending vibration of β-CH in the β-glycosidic bond (Kanwar et al., 2023). Compared with IDF, the peak intensity (*e.g.* 3410 cm^{-1} and 1072 cm^{-1}) of SDF increased significantly, which indicated that the active group (*e.g.* hydrogen bond) exposure of SDF was higher than IDF. The structural peculiarity of IDF and SDF contributed to the different hydration and rheological properties.

3.3. Hydration properties of IDF and SDF at different ratios

The hydration properties of DF include water retention capacity (WRC), water solubility index (WSI) and water swelling capacity (WSC), which are beneficial in reducing intestinal pressure, increasing the defecation rate of the body, and accelerating the elimination of toxins from the gastrointestinal tract (Carretta et al., 2021; Castillejo et al., 2006). As shown in Fig. 2A, the WRC of both IDF and SDF reached more than 5 g/g. The WRC of SDF was significantly ($P < 0.05$) lower than that of IDF, which might due to some of SDF was dissolved in the water (Fig. 2B). Thus, the measured WRC of SDF should be much lower than the real value. It was also found that the WRC of IDF-SDF mixtures decreased and the WSI of IDF-SDF mixtures significantly ($P < 0.05$) increased with the increase of SDF ratio (Fig. 2A-B). Moreover, the measured WRC values of DF mixed with different proportions were lower than the theoretical values calculated, which might be related to the dissolution of SDF in water.

SDF could swell to more than six times its original volume (Fig. 2C). The WSC of SDF was approximately twice that of IDF. Moreover, the WSC of IDF-SDF mixtures significantly ($P < 0.05$) increased with the increase of SDF ratio. It was related to the loose and porous structure of SDF and the exposure of active groups (Fig. 1). The measured WSC of

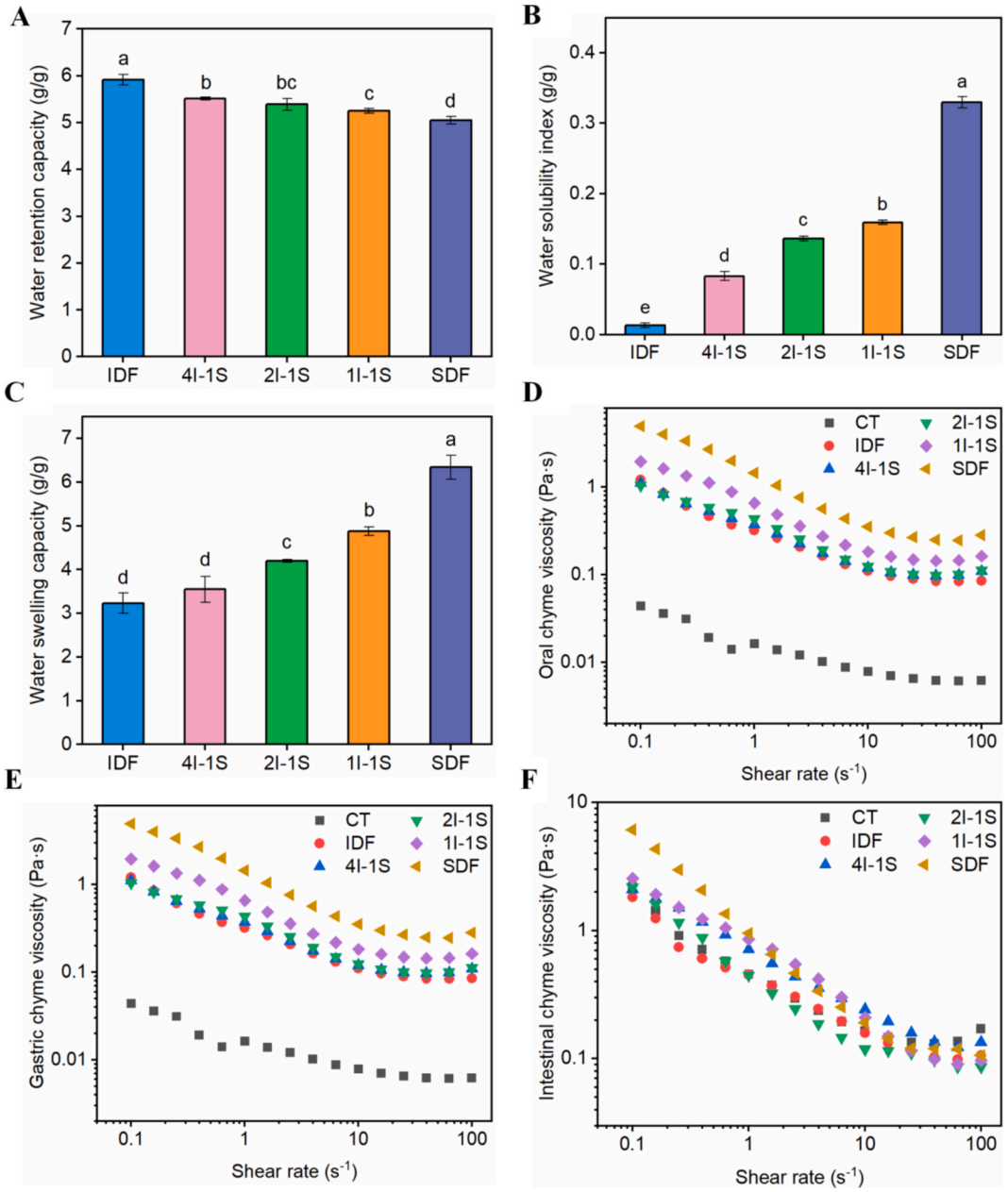

Fig. 2. Hydration properties (A-C) and rheological properties (D-E) of IDF and SDF at different ratios. Water retention capacity (A), Water solubility index (B), Water swelling capacity (C), Chyme viscosities of Oral phase (D), Gastric phase (E), and Small intestine phase (F). Values with different lowercase represent significant differences ($P < 0.05$).

different DF samples were similar to the theoretical WSC values calculated according to the ratios, indicating that the mixing of IDF and SDF did not change their respective WSC.

Compared with IDF, SDF had superior water solubility and water swelling capacity. Moreover, the mixtures of IDF and SDF at different ratios exhibited different hydration properties, which are important for relieving constipation and maintaining healthy intestinal function.

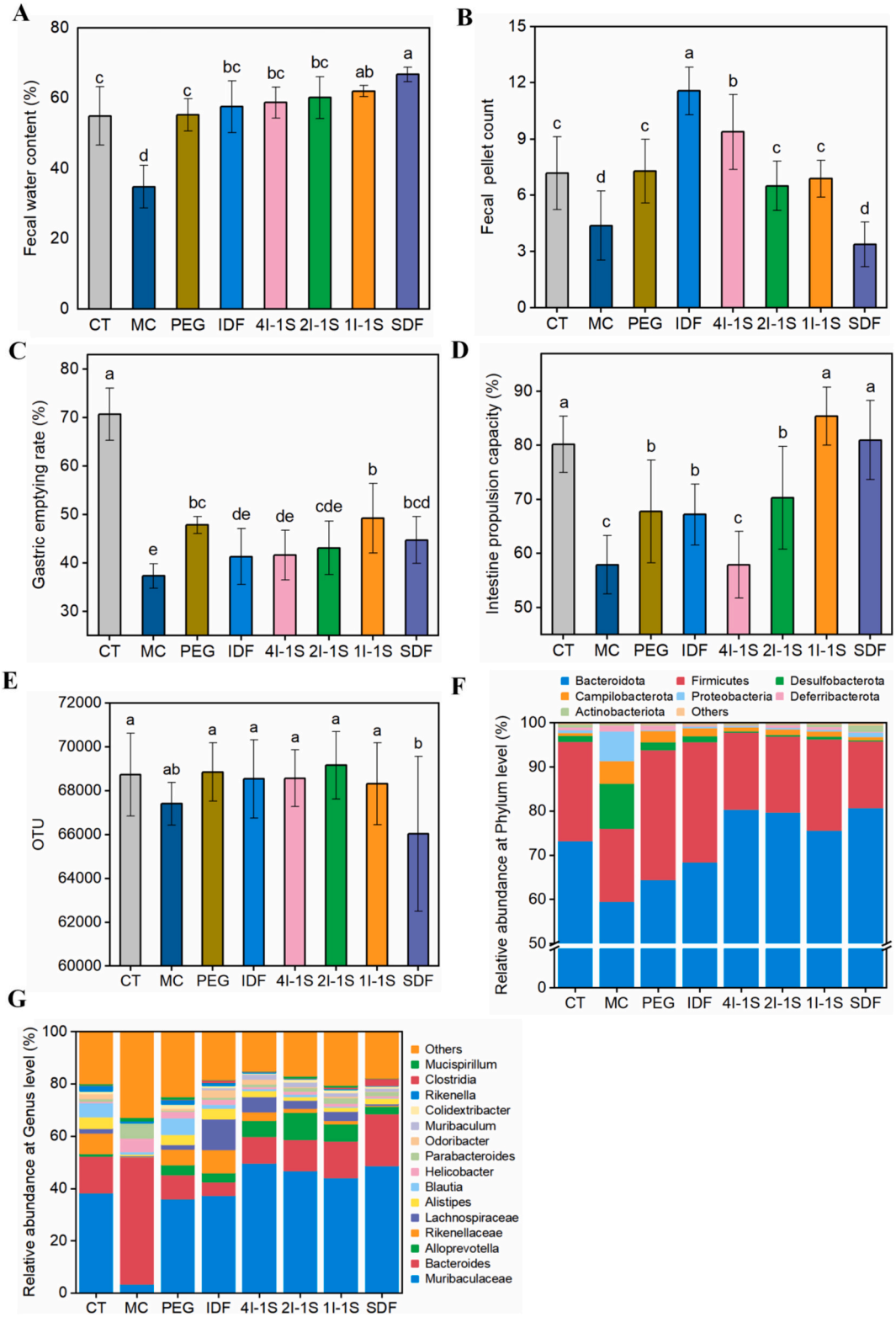

Fig. 3. Effects of different ratios of IDF and SDF on fecal related parameters (A-B), gastrointestinal motility (C—D) and Intestinal flora (*E*-G) in constipated mice. Fecal water content (A), Fecal pellet count (B), Gastric emptying rate (C), Small intestine propulsion capacity (D), OTU (E), Relative abundance at Phyum level (F), and Relative abundance at Genus level (F). Values with different lowercase represent significant differences ($P < 0.05$).

3.4. Rheological properties of SDF and IDF at different ratios during in vitro digestion

In the oral phase, the apparent viscosity of chyme decreased as the shear rate increased, indicating all chyme samples showed shear-thinning behavior. The viscosity of the high DF feed chyme was higher than that of normal standard feed chyme, which might be related to the strong water absorption capacity of DF. Meanwhile, the viscosity of high DF feed chyme gradually increased with the increase of SDF proportion. It might be due to the fact that SDF has higher water swelling capacity than IDF (Fig. 2D). The results were consistent with the study that the viscosity of oral chyme increased with the increase of β-glucan content in pig diet (Schop et al., 2020).

In the gastric phase (Fig. 2E), the apparent viscosity of chyme also decreased as the shear rate increased. Meanwhile, the decreasing rate of the chyme viscosity increased gradually with the increasing proportion of SDF, which indicated that the shear-thinning behavior was becoming more and more obvious. Compared with CT sample, the chyme viscosity of IDF sample slightly increased, and that of other high DF feed samples (4I—1S, 2I—1S, 1I—1S, and SDF) decreased. Among the five kinds of feed digesta supplemented with DF, the viscosity of digesta decreased with the increased SDF proportions. It might be because the lubrication effect of SDF improved the mobility of chyme, which might contribute to the gastric emptying.

The chyme in small intestine phase also showed shear-thinning behavior as oral and gastric phase. At low shear rates ($<10\ s^{-1}$), the viscosity of high DF feed chyme gradually increased with the increase of SDF proportion (Fig. 2F). However, there was no significant difference in the chyme viscosity between different samples at high shear rates ($10–100\ s^{-1}$). It should be noted that the intestinal digestion *in vitro* could avoid the effects of intestinal re-absorption function, and the changes of intestinal chyme viscosity *in vitro* might also predict the relationship between DF structure and digestive characteristics to a certain extent. The use of SDF alone might cause the risk of decreased chyme mobility in intestinal phase due to the excessive water absorption and high viscosity of SDF.

3.5. Fecal related parameters of constipated mice

As shown in Fig. 3A, the fecal water content of mice in MC group significantly ($P < 0.05$) decreased compared with CT. However, the fecal water content of mice returned to normal after treated with PEG or DF. This indicated that PEG or DF effectively increased the fecal water content of constipated mice and soften the feces, and thus relieved constipation. Among the five groups intervened with different ratios of DF, it could be observed that the fecal water content of the IDF, 4I—1S and 2I—1S groups, containing a higher proportion of IDF, were not significantly ($P > 0.05$) different from that of the PEG group. Meanwhile, the fecal water content tended to increase with the increase of SDF proportions, which might be related to the superior hydration characteristics of SDF.

Compared with CT, the fecal pellet count of MC significantly ($P < 0.05$) reduced (Fig. 3B). However, the fecal pellet counts significantly ($P < 0.05$) increased by intervention of PEG or DF, compared with MC. Meanwhile, the fecal pellet count decreased with the increase of SDF ratios. This might be due to the fact that SDF had a certain viscosity, which was better to maintain the integrity of the feces and makes them large and soft. This result was consistent with the study of constipated mice intervened with konjac glucomannan (Zhang, Zhong, et al., 2021). Moreover, the fecal pellet count of SDF group was significantly ($P < 0.05$) lower than that of CT group. This phenomenon also drew our attention to the potential risk of using the SDF alone to ameliorate constipation. Due to the excessive water-absorption and swelling of SDF, it resulted in large volume and low quantity of fecal, which could cause intestinal obstruction. In this respect, the more recommended ratios of IDF to SDF for constipation treatment was 2:1 or 1:1.

3.6. Gastrointestinal motility in constipated mice

The gastric emptying rate and small intestine propulsion capacity could be used to evaluate the gastrointestinal motility. After intervention of loperamide, the gastric emptying rate and small intestine propulsion capacity of MC group were significantly ($P < 0.05$) reduced, compared with the CT (Fig. 3C-D). It indicated that the gastrointestinal motility was insufficient in mice fed by gavage with loperamide, and the constipation model was successfully established. After treated with PEG, the gastric emptying rate and small intestine propulsion ability of mice significantly ($P < 0.05$) improved, and the constipation situation was relieved.

With the decrease of IDF proportions, the gastric emptying rate and small intestine propulsion capacity increased to varying degrees. As for IDF, 4I—1S and 2I—1S groups, the small intestinal propulsion capacity was partially improved, but the gastric emptying rate was not significantly ($P > 0.05$) different from that of MC. The metabolites produced by DF fermentation could regulate gastrointestinal motility through gastrointestinal hormones (gastrin and growth inhibitor) (Liu et al., 2019). The increased viscosity of SDF dissolved in water are more likely to delay gastric emptying and promote small intestinal peristalsis. IDF was less fermentable and viscous than SDF, so the increase in gastric emptying rate was not significant in the group treated with high IDF ratio (such as IDF, 4I—1S, 2I—1S group). Meanwhile, compared with MC, the gastric emptying rate and small intestinal propulsion capacity were all significantly ($P < 0.05$) improved in both 1I—1S and SDF groups. The small intestinal propulsion capacity in 1I—1S and SDF groups even returned back to normal levels, but the gastric emptying rate was still lower than CT group. The speed at which chyme moved through the digestive tract was related to its mobility, and a small amount of SDF could improve the mobility of chyme. When the ratio of IDF to SDF was 1:1, the mobility of food was the best, so the gastric emptying rate and small intestinal propulsion capacity of mice was the highest. However, a high proportion of SDF could result in excessive water absorption and expansion, as well as high viscosity, and thus led to a decrease in chyme mobility. Therefore, gastric emptying rate and small intestine propulsion capacity slightly decreased in SDF group, which was not significantly ($P > 0.05$) different from those in 1I—1S. The results of gastric emptying rate and small intestine propulsion capacity were consistent with the results of defecation related parameters.

3.7. Intestinal flora in constipated mice

The diversity of intestinal flora communities was assessed by 16S rDNA gene sequencing. After removing labels indicating low quality or no biological significance, a total of 4,645,806 valid labels were obtained from the 68 samples analyzed. Each sample covered an average of 68,321 valid labels. The average validity rate for all samples was 90.69 % (range of variation 85.59 % ~ 95.79 %). The mean commercial coverage for all samples was 98.49 % (range of variation 97.93 % ~ 99.69 %). These results indicated that the sequencing results represented the true picture of the bacteria.

Table 1
α-Diversity index of intestinal flora in mice.

Groups	Shannon	Simpson	Chao1
CT	7.36 ± 0.36^{b}	0.97 ± 0.01^{a}	3453 ± 308^{b}
MC	4.34 ± 0.72^{c}	0.87 ± 0.04^{b}	960 ± 341^{c}
PEG	7.60 ± 0.29^{ab}	0.98 ± 0.01^{a}	3507 ± 328^{b}
IDF	7.91 ± 0.29^{a}	0.98 ± 0.01^{a}	3937 ± 205^{a}
4I-1S	8.03 ± 0.49^{a}	0.98 ± 0.01^{a}	4078 ± 474^{a}
2I-1S	7.72 ± 0.47^{ab}	0.97 ± 0.01^{a}	3842 ± 410^{ab}
1I-1S	7.76 ± 0.53^{ab}	0.97 ± 0.03^{a}	3942 ± 408^{a}
SDF	7.59 ± 0.47^{ab}	0.97 ± 0.01^{a}	3539 ± 417^{b}

Data were presented as mean ± standard deviation. Values with different lowercase in the same column represent significant differences ($P < 0.05$).

The α-diversity of intestinal flora communities including Chao, Simpson, and Shannon indices are shown in Table 1. It was found that the α-diversity of the intestinal flora in MC was significantly ($P < 0.05$) lower than other groups. Among the DF treated groups, the α-diversity of intestinal flora tended to increase and then decrease with the decrease of IDF proportion, and it reached the highest in 4I—1S group.

The OTU results of intestinal flora in mice are shown in Fig. 3E. Compared with CT group, the OTU of intestinal flora in MC significantly ($P < 0.05$) reduced, which indicated that constipation reduced the OTU of intestinal microbiome in mice. Among the groups treated with DF, the 2I—1S group had the highest OTU, and the SDF group had the lowest OTU value. It indicated that IDF with a low dose of SDF promoted an increase in OTU of intestinal flora. However, excessive high proportion of SDF supplementation led to the decrease of OTU in intestinal flora. The decrease of OTU in SDF group might be related to the decrease of carbohydrate composition diversity and the change of intestinal movement (Castillejo et al., 2006; Hu et al., 2013; Jung et al., 2020). The main components of SDF samples were β-glucan (Table S1), while that of IDF were cellulose, hemicellulose and lignin (Saini et al., 2023).

The communities of intestinal flora are shown in Fig. 3F-G. Taxonomically, 25 phylums, 54 classes, 133 orders, 207 families, 364 genus and 537 species of microorganisms were identified in all mice. At the phylum level, the *Bacteroidetes* and *Firmicutes* were the main communities of intestinal microorganisms, which accounted for 76 % ~ 98 % (Fig. 3F). Compared with CT group, the abundance of *Bacteroides* and *Firmicutes* significantly ($P < 0.05$) decreased, while *Desulfobacterota*, *Campilobacterota*, and *Proteobacteria* increased in the MC group. The abundance of *Bacteroides and Firmicutes* was elevated in both groups after the intervention of DF. Meanwhile, the ratio of *Bacteroides* to *Firmicutes* decreased in IDF group, and increased in SDF group. At the genus level, the *Muribaculaceae, Alloprevotella, Rikenellaceae* and *Lachnospiraceae* significantly ($P < 0.05$) decreased, while *Bacteroides* significantly ($P < 0.05$) increased in MC group, compared with CT group (Fig. 3G). After the intervention of PEG and DF, the abundance of *Muribaculaceae, Alloprevotella, Rikenellaceae* and *Lachnospiraceae* significantly ($P < 0.05$) increased, compared with MC. The increase of *Muribaculaceae* was more pronounced in the presence of SDF, but the increase rate was independent of the SDF proportion. However, among the DF treated groups, the abundance of *Lachnospiraceae* tended to decrease with the increase of SDF proportion. The highest and the lowest values of *Lachnospiraceae* abundance were found in IDF and SDF group, respectively. The increase of probiotics caused by single use of IDF or SDF could inhibit the growth and reproduction of other microorganisms in the intestinal tract, especially harmful microorganisms. However, the combined use of SDF and IDF in a certain proportion was more beneficial to the diversity of intestinal flora and the growth of probiotics than the use of SDF or IDF alone.

3.8. Effect of different ratios of IDF to SDF on SCFAs in constipated mice

SCFAs could provide energy for intestine epithelial cell, improve the function of intestinal barrier, increase electrolyte and water absorption, and promote intestine peristalsis, which can be produced by fermenting DF. As shown in Table 2, the content of all types of SCFAs in MC group significantly ($P < 0.05$) decreased after treated with loperamide, compared with CT group. However, all types of SCFAs increased after the intervention of PEG and DF, compared with MC. As for the five groups treated with DF, the total amount of SCFAs increased with the increase of SDF ratios, and the 1I—1S group was the highest. This result could explain the findings that the mice in 1I—1S group had higher small intestinal propulsive capacity. Moreover, there was no significant ($P > 0.05$) difference between 1I-IS and SDF group, which indicated that the moderate amount of SDF was beneficial to improve the metabolic production of SCFAs. Acetic acid, propionic acid and butyric acid were the main species of SCFAs, which accounted for about 95 % of the total SCFAs. It was found that the contents of acetic acid (755.04 μg/mL), propionic acid (174.54 μg/mL) and butyric acid (141.19 μg/mL) were the highest in the SDF group, 1I—1S group and IDF group, respectively. It also indicated that SDF was more favorable for the production of acetic acid, while IDF was more favorable for the production of butyric acid. It also indicated that SDF was more favorable for the production of acetic acid, while IDF was more favorable for the production of butyric acid. It might be related to the carbohydrate composition of DF samples and the growth of gut microbes (Hu et al., 2013; Müller et al., 2020; Yang et al., 2013). Therefore, the mixed use of SDF and IDF in a certain proportion was more beneficial to the production of SCFAs than the use of SDF or IDF alone.

3.9. Effect of different ratios of IDF to SDF on gastrointestinal hormones in constipated mice

Gastrointestinal hormones, including MTL, Ach, and 5-HT, could jointly regulate the contraction and relaxation of smooth muscle, as well as enhance gastrointestinal peristalsis and propulsion (Zanzer et al., 2018). Compared with CT group, the content of MLT and 5-HT in MC group significantly ($P < 0.05$) decreased, while the concentration of NO significantly ($P < 0.05$) increased, after treated with loperamide

Table 3
Gastrointestinal hormones in constipated mice.

	MTL (pg·mL^{-1})	Ach (pg·mL^{-1})	5-HT (pg·mL^{-1})	NO (pg·mL^{-1})
CT	56.52 ± 6.8^{a}	51.19 ± 3.52^{ab}	152.33 ± 23.14^{cd}	29.27 ± 8.07^{b}
MC	34.71 ± 2.76^{d}	47.28 ± 5.24^{b}	130.08 ± 12.76^{d}	37.38 ± 11.05^{a}
PEG	43.48 ± 5.15^{bc}	50.48 ± 5.02^{ab}	186.87 ± 31.78^{a}	28.23 ± 4.56^{bc}
IDF	40.16 ± 3.08^{bcd}	48.82 ± 2.49^{ab}	164.69 ± 26.2^{abc}	29.32 ± 2.32^{b}
4I-1S	37.51 ± 6.91^{cd}	55.64 ± 11.16^{ab}	175.76 ± 30.63^{abc}	25.26 ± 3.11^{bc}
2I-1S	35.22 ± 4.55^{d}	52.45 ± 5.43^{ab}	184.29 ± 17.07^{ab}	24.27 ± 2.65^{bc}
1I-1S	45.10 ± 4.79^{b}	56.64 ± 7.69^{a}	191.75 ± 14.45^{a}	21.39 ± 4.6^{c}
SDF	43.49 ± 7.02^{bc}	47.98 ± 10.60^{ab}	155.76 ± 14.53^{bcd}	13.37 ± 4.13^{d}

Data were presented as mean ± standard deviation. Values with different lowercase in the same column represent significant differences ($P < 0.05$).

Table 2
Effect of different ratios of IDF to SDF on SCFA content in constipated mice (μg/mL).

Groups	Acetic acid	Propionic acid	Butyric acid	Isobutyric acid	Isovaleric acid	Valeric acid
CT	755.66 ± 49.10^{a}	134.45 ± 12.22^{bc}	134.11 ± 12.92^{a}	16.02 ± 1.56^{ab}	20.12 ± 1.47^{b}	21.37 ± 2.82^{a}
MC	452.38 ± 28.66^{c}	101.42 ± 12.40^{d}	23.87 ± 5.59^{d}	7.01 ± 1.30^{c}	8.92 ± 2.38^{d}	7.20 ± 4.90^{d}
PEG	696.82 ± 131.56^{ab}	134.50 ± 30.68^{bc}	129.87 ± 22.57^{a}	15.89 ± 2.96^{ab}	17.84 ± 3.51^{bc}	18.42 ± 3.57^{ab}
IDF	711.93 ± 73.70^{ab}	123.09 ± 4.89^{cd}	141.19 ± 17.80^{a}	14.43 ± 0.92^{ab}	15.29 ± 2.00^{c}	15.76 ± 2.27^{b}
4I-1S	738.48 ± 106.55^{ab}	130.98 ± 22.03^{bcd}	119.54 ± 17.11^{ab}	15.02 ± 1.74^{ab}	17.04 ± 2.57^{bc}	14.56 ± 1.34^{bc}
2I-1S	628.24 ± 108.62^{b}	135.71 ± 21.32^{bc}	72.34 ± 18.19^{c}	13.20 ± 3.06^{b}	14.30 ± 2.86^{c}	11.14 ± 2.66^{cd}
1I-1S	710.34 ± 84.77^{ab}	174.54 ± 42.24^{a}	95.98 ± 34.62^{bc}	16.49 ± 4.65^{ab}	20.14 ± 4.74^{b}	17.91 ± 5.67^{ab}
SDF	755.04 ± 100.26^{a}	157.48 ± 25.62^{ab}	71.94 ± 23.98^{c}	17.94 ± 3.07^{a}	25.11 ± 4.17^{a}	16.64 ± 4.93^{b}

Data were presented as mean ± standard deviation. Values with different lowercase in the same column represent significant differences ($P < 0.05$).

(Table 3). NO is an endogenous diastolic molecule that causes smooth muscle relaxation. When the NO levels are too high, contractile dysfunction occurs and constipation symptoms are exacerbated (Katsirma et al., 2021; Sharma & Rao, 2017). It indicated that the contraction of smooth muscle and the peristalsis of gastrointestinal tract in constipated mice were weakened, which resulted in relaxed smooth muscle and impaired intestine contractile function. After the intervention of PEG, the contents of MTL and 5-HT significantly ($P < 0.05$) increased and the concentration of NO significantly ($P < 0.05$) decreased, which indicated that the gastrointestinal motility of mice was partially restored. As for the five DF-supplemented groups, the concentration of NO decreased with the increase of SDF proportions. The content of 5-HT increased firstly and then decreased with the increase of SDF proportions, which reached the maximum value at IDF: SDF = 1:1 (1I-IS group). Ach and MTL did not differ significantly ($P > 0.05$) among the groups treated with different proportions of DF, but the 1I—1S group had the highest content of Ach and MTL. The effects of different ratios of IDF to SDF on MTL and 5-HT content were consistent with the results of gastric emptying rate and small intestine propulsive capacity. The value of MTL was positively correlated with gastric emptying rate ($r = 0.946$, $P < 0.01$) and small intestine propulsive capacity ($r = 0.69$, $P > 0.05$), respectively.

4. Conclusion

The underlying mechanisms of IDF and SDF at different ratios on constipation induced by loperamide was studied through hydration properties, chyme rheological properties, gastrointestinal motility, intestinal flora, short chain fatty acid, and gastrointestinal hormone. Compared with IDF, the fibrous structure of SDF was looser and more porous, and the active group (*e.g.* hydrogen bond) exposure of SDF was higher. *In vitro,* with the increase of the proportion of SDF, the WSI, WSC and oral phase viscosity of DF mixture significantly increased, while the WRC and gastric phase viscosity significantly decreased. When the ratios of IDF to SDF was 2:1 or 1:1, the fecal water content and fecal pellet count of constipated mice reached the normal level. When the ratio of IDF to SDF was 1:1, the gastric emptying rate and small intestine propulsion capacity reached the highest. The use of SDF alone led to a decrease in chyme mobility and gut microbiome diversity. SDF was more favorable for the production of acetic acid, while IDF was more favorable for the production of butyric acid. The total amount of SCFAs and gastrointestinal hormones secretion of MTL, Ach, and 5-HT were the highest when the ratio of IDF to SDF was 1:1. Our studies showed that the combination of IDF and SDF in a certain proportion was a potential choice of dietary therapy products for constipation, and the best was 1:1. It would overcome the potential disadvantages of using IDF and SDF alone. The effect of different ratios of IDF to SDF on immune and inflammatory responses, as well as the relationship between glucose/ lipid metabolism and intestinal flora in constipation mouse model need to be further studied.

CRediT authorship contribution statement

Lijuan Wang: Writing – original draft, Software, Methodology, Investigation. **Jiaxin Wang:** Validation, Formal analysis. **Jialin Wang:** Visualization, Software. **Zicong Guo:** Validation, Software. **Zaigui Li:** Writing – review & editing, Validation. **Ju Qiu:** Writing – review & editing, Supervision, Resources, Project administration, Funding acquisition. **Lili Wang:** Writing – review & editing, Supervision, Resources, Project administration, Funding acquisition.

Declaration of competing interest

The authors declare that they have no known competing financial interests or personal relationships that could have appeared to influence the work reported in this paper.

Data availability

The authors are unable or have chosen not to specify which data has been used.

Acknowledgements

This work was supported by the National Key Research and Development Plan (2022YFF1100500, 2022YFF1100504-04, 2022YFF1100501-03), Yimeng Innovation and Entrepreneurship Leading Talents (2022), Shanxi Province Key Research and Development Plan (202102140601014), and Central Public-interest Scientific Institution Basal Research Fund (No.S2022JBKY-06).

Appendix A. Supplementary data

Supplementary data to this article can be found online at https://doi.org/10.1016/j.fochx.2024.101996.

References

American Association of Cereal Chemists (AACC). (2010). *Approved methods of the AACC* (11th ed.). St Paul, MN, USA: AACC International. https://doi.org/10.1094/AACCIntMethod

Bae, S. H. (2014). Diets for constipation. *Pediatric Gastroenterology, Hepatology & Nutrition, 17*, 203–208. https://doi.org/10.5223/pghn.2014.17.4.203

Bharucha, A. E., & Lacy, B. E. (2020). Mechanisms, evaluation, and management of chronic constipation. *Gastroenterology, 158*, 1232–1249. https://doi.org/10.1053/j.gastro.2019.12.034

Carretta, M. D., Quiroga, J., López, R., Hidalgo, M. A., & Burgos, R. A. (2021). Participation of short-chain fatty acids and their receptors in gut inflammation and colon cancer. *Frontiers in Physiology, 12*, Article 662739. https://doi.org/10.3389/fphys.2021.662739

Castillejo, G., Bullo, M., Anguera, A., Escribano, J., & Salas-Salvado, J. (2006). A controlled, randomized, double-blind trial to evaluate the effect of a supplement of cocoa husk that is rich in dietary fiber on colonic transit in constipated pediatric patients. *Pediatrics, 118*, e641–e648. https://doi.org/10.1542/peds.2006-0090

Chan, A. O., Leung, G., Tong, T., & Wong, N. Y. H. (2007). Increasing dietary fiber intake in terms of kiwifruit improves constipation in Chinese patients. *World Journal of Gastroenterology, 13*, 4771–4775. https://doi.org/10.3748/wjg.v13.i35.4771

Crowe, M. S., & Kinsey, S. G. (2017). MAGL inhibition modulates gastric secretion and motility following NSAID exposure in mice. *European Journal of Pharmacology, 807*, 198–204. https://doi.org/10.1016/j.ejphar.2017.05.006

Hu, J. L., Nie, S. P., Li, C., & Xie, M. Y. (2013). *In vitro* fermentation of polysaccharide from the seeds of *Plantago asiatica* L. by human fecal microbiota. *Food Hydrocolloids, 33*, 384–392. https://doi.org/10.1016/j.foodhyd.2013.04.006

Jiménez-Escrig, A., & Sánchez-Muniz, F. J. (2000). Dietary fibre from edible seaweeds: Chemical structure, physicochemical properties and effects on cholesterol metabolism. *Nutrition Research, 20*, 585–598. https://doi.org/10.1016/S0271-5317(00)00149-4

Jung, S. J., Oh, M. R., Park, S. H., & Chae, S. W. (2020). Effects of rice-based and wheat-based diets on bowel movements in young Korean women with functional constipation. *European Journal of Clinical Nutrition, 74*, 1565–1575. https://doi.org/10.1038/s41430-020-0636-1

Kanwar, P., Yadav, R. B., & Yadav, B. S. (2023). Cross-linking, carboxymethylation and hydroxypropylation treatment to sorghum dietary fiber: Effect on physicochemical, micro structural and thermal properties. *International Journal of Biological Macromolecules, 233*, Article 123638. https://doi.org/10.1016/j.ijbiomac.2023.123638

Katsirma, Z., Dimidi, E., Rodriguez-Mateos, A., & Whelan, K. (2021). Fruits and their impact on the gut microbiota, gut motility and constipation. *Food & Function, 12*, 8850–8866. https://doi.org/10.1039/d1fo01125a

Kurek, M. A., Karp, S., Wyrwisz, J., & Niu, Y. (2018). Physicochemical properties of dietary fibers extracted from gluten-free sources: Quinoa (*Chenopodium quinoa*), amaranth (*Amaranthus caudatus*) and millet (*Panicum miliaceum*). *Food Hydrocolloids, 85*, 321–330. https://doi.org/10.1016/j.foodhyd.2018.07.021

Li, Y., Wang, L. J., Wang, H. R., Li, Z. G., Qiu, J., & Wang, L. L. (2022). Correlation of microstructure, pore characteristics and hydration properties of wheat bran modified by airflow impact mill. *Innovative Food Science & Emerging Technologies, 77*, Article 102977. https://doi.org/10.1016/j.ifset.2022.102977

Liu, X. Y., Chen, S., Yan, Q. J., Li, Y. X., & Jiang, Z. Q. (2019). Effect of Konjac mannan oligosaccharides on diphenoxylate-induced constipation in mice. *Journal of Functional Foods, 57*, 399–407. https://doi.org/10.1016/j.jff.2019.04.036

Mäkelä, N., Brinck, O., & Sontag-Strohm, T. (2020). Viscosity of β-glucan from oat products at the intestinal phase of the gastrointestinal model. *Food Hydrocolloids, 100*, Article 105422. https://doi.org/10.1016/j.foodhyd.2019.105422

Mälkki, Y., & Virtanen, E. (2001). Gastrointestinal effects of oat bran and oat gum: A review. *LWT - Food Science and Technology, 34*, 337–347. https://doi.org/10.1006/fstl.2001.0795

Müller, M., Hermes, G. D. A., Emanuel, E. C., Holst, J. J., Zoetendal, E. G., Smidt, H., … Blaak, E. E. (2020). Effect of wheat bran derived prebiotic supplementation on gastrointestinal transit, gut microbiota, and metabolic health: A randomized controlled trial in healthy adults with a slow gut transit. *Gut Microbes, 12*, Article 1704141. https://doi.org/10.1080/19490976.2019.1704141

Novick, J., Miner, P., Krause, R., Glebas, K., Bliesath, H., Ligozio, G., Rüegg, P., & Lefkowitz, M. (2002). A randomized, double-blind, placebo-controlled trial of tegaserod in female patients suffering from irritable bowel syndrome with constipation. *Alimentary Pharmacology & Therapeutics, 16*, 1877–1888. https://doi.org/10.1046/j.1365-2036.2002.01372.x

Rezvani, Z., & Goli, S. A. H. (2023). Fabrication, physicochemical properties and structural characteristics of nanoparticles from carrot pomace and its insoluble dietary fiber. *Food Hydrocolloids, 145*, Article 109131. https://doi.org/10.1016/j.foodhyd.2023.109131

Rosa-Sibakov, N., Poutanen, K., & Micard, V. (2015). How does wheat grain, bran and aleurone structure impact their nutritional and technological properties? *Trends in Food Science & Technology, 41*, 118–134. https://doi.org/10.1016/j.tifs.2014.10.003

Saini, P., Islam, M., Das, R., Shekhar, S., Sinha, A. S. K., & Prasad, K. (2023). Wheat bran as potential source of dietary fiber: Prospects and challenges. *Journal of Food Composition and Analysis, 116*, Article 105030. https://doi.org/10.1016/j.jfca.2022.105030

Schop, M., Jansman, A. J. M., de Vries, S., & Gerrits, W. J. J. (2020). Increased diet viscosity by oat β-glucans decreases the passage rate of liquids in the stomach and affects digesta physicochemical properties in growing pigs. *Animal, 14*, 269–276. https://doi.org/10.1017/S1751731119001824

Sharma, A., & Rao, S. (2017). Constipation: Pathophysiology and current therapeutic approaches. *Handbook of Experimental Pharmacology, 239*, 59–74. https://doi.org/10.1007/164_2016_111

Slavin, J. (2013). Fiber and prebiotics: Mechanisms and health benefits. *Nutrients, 5*(4), 1417–1435. https://doi.org/10.3390/nu5041417

Sowbhagya, H. B., Suma, P. F., Mahadevamma, S., & Tharanathan, R. N. (2007). Spent residue from cumin – A potential source of dietary fiber. *Food Chemistry, 104*, 1220–1225. https://doi.org/10.1016/j.foodchem.2007.01.066

Sumida, K., Molnar, M. Z., Potukuchi, P. K., Thomas, F., Lu, J. L., Yamagata, K., … Kovesdy, C. P. (2019). Constipation and risk of death and cardiovascular events. *Atherosclerosis, 281*, 114–120. https://doi.org/10.1016/j.atherosclerosis.2018.12.021

Wang, L. J., Wang, L. B., Wang, A. L., Qiu, J., & Li, Z. G. (2021). Effects of superheated steam on starch structure and physicochemical properties of buckwheat flour during storage. *Journal of Cereal Science, 99*, Article 103221. https://doi.org/10.1016/j.jcs.2021.103221

Wang, L. L., Hu, L. J., Xu, Q., Jiang, T., Fang, S. G., Wang, G., … C, W.. (2017). Bifidobacteria exert species-specific effects on constipation in BALB/c mice. *Food & Function, 8*, 3587–3600. https://doi.org/10.1039/c6fo01641c

Yang, J., Martínez, I., Walter, J., Keshavarzian, A., & Rose, D. J. (2013). *In vitro* characterization of the impact of selected dietary fibers on fecal microbiota composition and short chain fatty acid production. *Anaerobe, 23*, 74–81. https://doi.org/10.1016/j.anaerobe.2013.06.012

Zanzer, Y. C., Plaza, M., Dougkas, A., Turner, C., & Östman, E. (2018). Black pepper-based beverage induced appetite-suppressing effects without altering postprandial glycaemia, gut and thyroid hormones or gastrointestinal well-being: A randomized crossover study in healthy subjects. *Food & Function, 10*, 1039. https://doi.org/10.1039/c7fo01715d

Zhang, Q., Zhong, D. A., Ren, Y. Y., Meng, Z. K., Pegg, R. B., & Zhong, G. (2021). Effect of konjac glucomannan on metabolites in the stomach, small intestine and large intestine of constipated mice and prediction of the KEGG pathway. *Food & Function, 12*, 3044–3056. https://doi.org/10.1039/d0fo02682d

Further-reading

Zhang, X. Y., Yang, H. B., Zheng, J. P., Jiang, N., Sun, G. J., Bao, X. K., … Liu, H. T. (2021). Chitosan oligosaccharides attenuate loperamide-induced constipation through regulation of gut microbiota in mice. *Carbohydrate Polymers, 253*, Article 117218. https://doi.org/10.1016/j.carbpol.2020.117218